Published in IET Communications
Received on 6th March 2008
Revised on 26th November 2008
doi: 10.1049/iet-com.2008.0133

ISSN 1751-8628

Time-domain equalisation for discrete multi-tone transceivers: new results and performance analysis

W.R. Wu C.F. Lee Y.F. Chen

Department of Communication Engineering, National Chiao Tung University, Hsinchu 300, Taiwan
E-mail: jefflee.cm89g@nctu.edu.tw

Abstract: The time-domain equaliser (TEQ) is a commonly used device to shorten the channel impulse response in a discrete multitone (DMT) receiver. Many methods have been proposed to design the TEQ with a capacity maximisation criterion. An implicit assumption used by existing methods is that circular convolution can be conducted for the noise signal and the TEQ. This assumption is not valid because the noise vector, observed in a DMT symbol, does not have a cyclic prefix. A similar assumption is also made for the residual inter-symbol interference (ISI) signal. Because of these invalid assumptions, the TEQ-filtered noise and residual ISI powers in each subcarrier were not properly evaluated. As a result, optimum solutions derived are not actually optimal. This paper attempts to resolve this problem. We first analyse the statistical properties of the TEQ-filtered noise signal and the residual ISI signal in detail, and derive precise formulae for the calculation of the TEQ-filtered noise and residual ISI powers. Then, we re-formulate the capacity maximisation criterion to design the true optimum TEQ. Simulations show that the proposed method outperforms the existing ones, and its performance closely approaches the theoretical upper bound.

1 Introduction

Digital subscriber line (DSL) is an advanced technology providing high-speed data transmission via the twisted pair wire for broadband internet delivery. The discrete multitone (DMT), a multicarrier modulation technique [1, 2], has become the standard for transmission line code for various DSL systems, such as asymmetric DSL (ADSL) [3–5] and very high speed DSL (VDSL) [6]. The DMT divides the available signal band into many subchannels and generates a subcarrier for data transmission in each subchannel. The data rate for each subcarrier is maximised with a bit loading algorithm such that the bandwidth can be used in an efficient way.

The DSL channel is known to have a low-pass characteristic. As a result, the impulse response is usually quite long. The inter-symbol interference (ISI) is then a major impairment in a DMT system. To solve the problem, the idea of cyclic prefix (CP) is introduced. However, the CP will reduce the data rate and a large-size CP is not desirable. A compromising approach is to use a time-domain equaliser (TEQ) in the receiver side such that the channel response can be shortened and a smaller CP is applicable. The design of the TEQ is a critical problem in DMT systems.

Many methods have been proposed to solve the TEQ design problem [7–22]. A conventional method uses the minimum mean squared error (MMSE) algorithm [7, 8], which minimises the mean squared error between two responses, one with the TEQ shortened impulse response, and the other a desired impulse response. Treating the TEQ design as a pure channel shortening problem, the work in [9] proposes a criterion to maximise the shortening signal-to-noise (SNR) ratio (SSNR), defined as the ratio of the energy of the TEQ shortened response inside and outside the CP range. This method was referred to as the maximised SSNR (MSSNR) method. Another shortening method, minimising the channel delay spread, has also been proposed [14–16]. Note that all these methods do

not consider the impact of the TEQ on channel capacity, and they are not optimal in general.

The work in [10] first considered capacity maximisation in the TEQ design. With a geometric SNR maximisation, a constrained non-linear optimisation problem was obtained. As a closed-form solution did not exist, some numerical method was used in [10]. One drawback to this work is that the residual ISI effect was not considered. A method referred to as maximum bit rate (MBR) [12] was then proposed, taking both residual ISI and channel noise into account. To reduce the computational complexity, a suboptimum method called minimum ISI (min-ISI), which performed similarly to the MBR method, was also developed. Another MBR related method was suggested in [19]. It is known that when the maximum excess delay exceeds the CP range, inter-carrier interference (ICI) will occur in DMT systems. Thus, the residual ISI will induce ICI, and this problem was examined in [11]. It was found that the aforementioned methods shared a common mathematical framework based on the maximisation of a product of generalised Rayleigh quotients [17].

The methods mentioned above conducted the TEQ design entirely in the time domain. Another approach, treating the problem in the frequency domain, was proposed in [18]. This method, referred to as per-tone equalisation (PTEQ), allows an equaliser designed for the signal in each tone. By taking the computational advantage of fast Fourier transform (FFT), TEQ filtering operations can be effectively implemented in the discrete Fourier transform (DFT) domain. It was shown that the PTEQ scheme can outperform conventional TEQ schemes. However, the PTEQ requires a large quantity of memory for storage and potentially greater computational complexity [17]. Another method, called subsymbol equalisation [20], also designed the TEQ in the frequency domain. It used the conventional zero-forcing frequency domain equaliser to obtain the equalised time-domain signal. The drawback of this approach is that it is only applicable to a certain type of channels.

The MBR design method [12] has proved to be an effective TEQ design method. Unfortunately, we have found that in the derivation of the MBR method, the TEQ-filtered noise and the ISI power were not properly evaluated. As a result, the MBR method, claimed to be optimal, is not truly optimal. This is because of the assumption made in [12] (also in [10]) that the DFT of the TEQ-filtered noise is equal to the DFT of the TEQ response multiplied by that of the noise sequence (in a DMT symbol). This is equivalent to saying that the TEQ-filtered noise is obtained with a circular convolution of the TEQ response and the noise sequence. However, the noise sequence does not have a CP, and the TEQ-filtered noise corresponds to a linear convolution of the TEQ response and the noise sequence, instead of a circular convolution. This problem was first discovered by us [21, 22], and it was also briefly mentioned in a recently published work [20] (no detailed discussions and derivations were reported). A similar assumption was also made for the residual ISI [12]. Note that the residual ISI is the ISI response outside the CP range. As a result, the residual ISI cannot be obtained with a circular convolution of the input signal and the residual ISI response. This paper attempts to resolve the problems not considered previously. We present a detailed analysis of the TEQ-filtered noise and residual ISI in a DMT system, and derive correct formulae for the calculation of the noise and residual ISI powers. It turns out that these powers are larger than those previously calculated [10, 12]. With the analytic results, we further re-formulate the capacity function, and then propose a new method for TEQ design.

The paper is organised as follows. In Section 2, we build the signal model and briefly review the TEQ design method in [12]. In Section 3, we analyse the impact of the noise and residual ISI to the TEQ design, and derive correct formulae for the calculation of noise and residual ISI powers. In Section 4, we re-formulate the conventionally used cost function and propose a new TEQ design method. Section 5 gives simulation results, and finally conclusions are drawn in Section 6.

2 Background

First we define variables and symbols used frequently throughout this work. Let M be the DFT size, L the CP length, $K = M + L$ the DMT symbol length, I the channel length, and N the TEQ length. In addition, let n be the signal index, i the DMT symbol index, both in the time domain, and k the subchannel index in the DFT domain, where $0 \leq k \leq (M/2) - 1$. Moreover, let $*$ be the linear convolution operation, $\bullet$ the element-by-element vector multiplication, and $\circledast$ the M-point circular convolution operation. Furthermore, denote $[\cdot]^{\mathrm{T}}$, $[\cdot]^{*}$, and $[\cdot]^{\mathrm{H}}$ as the transpose, the complex conjugate, and the Hermitian operations for a vector or matrix, respectively. Denote $\mathbf{0}_p$ as the $p \times 1$ zero column vector, $\mathbf{1}_p$ the $p \times 1$ unity column vector, $\mathbf{0}_{p\times q}$ the $p \times q$ zero matrix, and $\boldsymbol{I}_p$ the $p \times p$ identity matrix. Moreover, we use diag[·] to denote either the vector formed by the diagonal elements of a matrix, or a diagonal matrix formed by a vector. For notational convenience, we denote $\lfloor \boldsymbol{a} \rceil^2 = \boldsymbol{a}\boldsymbol{a}^{\mathrm{H}}$, and $\langle \boldsymbol{a} \rangle^2 = \mathrm{diag}[\boldsymbol{a}\boldsymbol{a}^{\mathrm{H}}]$, where $\boldsymbol{a}$ is a vector. Note that $\lfloor \boldsymbol{a} \rceil^2$ is a matrix while $\langle \boldsymbol{a} \rangle^2$ is a vector. Also, these operations are applicable to matrices.

2.1 Signal model

A common model of a DMT system with the TEQ design is shown in Fig. 1. At the DMT transmitter side, we denote the ith transmitted data symbol as

$$\tilde{\boldsymbol{d}}_i = [\tilde{d}_i(0), \ldots, \tilde{d}_i(M-1)]^{\mathrm{T}}$$

where $\tilde{d}_i(k)$ is the $(k+1)$th element of $\tilde{\boldsymbol{d}}_i$. Taking the M-point inverse DFT (M-IDFT) of $\tilde{\boldsymbol{d}}_i$, we can then

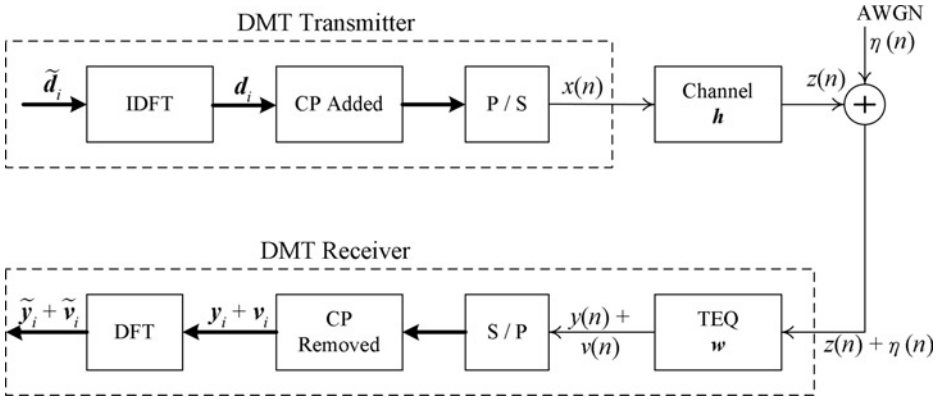

Figure 1 *A DMT model for TEQ design*

obtain the corresponding time domain signal, denoted as $\boldsymbol{d}_i$. Then,

$$\boldsymbol{d}_i = [d_i(0), \ldots, d_i(M-1)]^{\mathrm{T}} = \frac{1}{M}\boldsymbol{F}^{\mathrm{H}}\tilde{\boldsymbol{d}}_i$$

where $\boldsymbol{F}$ is an $M \times M$ DFT matrix. Let $\alpha = e^{-j2\pi/M}$ and

$$\boldsymbol{f}(k) = \left[1, \alpha^k, \ldots, \alpha^{(M-1)k}\right]^{\mathrm{T}}$$

We then have

$$\boldsymbol{F} = \left[\boldsymbol{f}(0), \boldsymbol{f}(1), \ldots, \boldsymbol{f}(M-1)\right]$$

Subsequently, appending the CP and conducting the parallel-to-serial conversion, we obtain the transmitted signal $x(n)$. Here, $n = iK + l$, and

$$\begin{cases} x(iK+l) = d_i(l+M-L), & \text{for } 0 \le l \le L-1 \\ x(iK+l) = d_i(l-L), & \text{for } L \le l \le K-1 \end{cases}$$

where $d_i(l)$ is the $(l+1)$th element of $\boldsymbol{d}_i$. The signal $x(n)$ is then transmitted over a finite impulse response (FIR) channel and corrupted by additive white Gaussian noise (AWGN).

Let the channel response be represented as

$$\boldsymbol{h} = [h(0), \ldots, h(I-1)]^{\mathrm{T}}$$

and the AWGN as $\eta(n)$. Denote the noise-free channel output signal as $z(n)$. Then

$$z(n) = x(n) * h(n)$$

At the receiver side, both $z(n)$ and $\eta(n)$ are first filtered by an N-tap TEQ. Let the TEQ coefficients be denoted as

$$\boldsymbol{w} = [w(0), \ldots, w(N-1)]^{\mathrm{T}}$$

Also, let the corresponding TEQ-filtered output of $z(n)$ and that of the channel noise be $y(n)$ and $v(n)$, respectively. Thus, $y(n) = z(n) * w(n)$ and $v(n) = \eta(n) * w(n)$. Moreover, let the optimum delay be Δ. Performing the serial-to-parallel conversion and removing the CP, we can obtain the ith received signal-only DMT symbol as

$$\boldsymbol{y}_i = \left[y(iK+\Delta+L), \ldots, y(iK+\Delta+K-1)\right]^{\mathrm{T}}$$

With the M-DFT operation, we have

$$\tilde{\boldsymbol{y}}_i = [\tilde{y}_i(0), \ldots, \tilde{y}_i(M-1)]^{\mathrm{T}} = \boldsymbol{F}\boldsymbol{y}_i$$

where $\tilde{y}_i(k)$ is the $(k+1)$th element of $\tilde{\boldsymbol{y}}_i$. Let the corresponding ith noise vector at the TEQ input and output be

$$\boldsymbol{\eta}_i = [\eta(iK+\Delta+L), \ldots, \eta(iK+\Delta+K-1)]^{\mathrm{T}}$$

and

$$\boldsymbol{v}_i = [v(iK+\Delta+L), \ldots, v(iK+\Delta+K-1)]^{\mathrm{T}}$$

respectively. We can obtain their M-DFT transformed vectors as

$$\tilde{\boldsymbol{\eta}}_i = [\tilde{\eta}_i(0), \ldots, \tilde{\eta}_i(M-1)]^{\mathrm{T}} = \boldsymbol{F}\boldsymbol{\eta}_i$$

and

$$\tilde{\boldsymbol{v}}_i = [\tilde{v}_i(0), \ldots, \tilde{v}_i(M-1)]^{\mathrm{T}} = \boldsymbol{F}\boldsymbol{v}_i$$

respectively.

From Fig. 1, we can see that the transmitted signal $x(n)$ passes the channel $h(n)$ and the TEQ filter $w(n)$. Let $g(n)$ be the equivalent channel response where

$$g(n) = h(n) * w(n)$$

and the length of $g(n)$ be J where $J = I + N - 1$. Here, we assume that $J < M$. Let

$$\boldsymbol{g} = \left[g(0), g(1), \ldots, g(J-1)\right]^{\mathrm{T}}$$

doi: 10.1049/iet-com.2008.0133

Fig. 2*a* shows the effective channel of a DMT system. We can then decompose $\boldsymbol{g}$ into two parts

$$\boldsymbol{g} = \boldsymbol{g}_{\mathrm{S}} + \boldsymbol{g}_{\mathrm{I}}$$

The first part

$$\boldsymbol{g}_{\mathrm{S}} = \left[\boldsymbol{0}_{\Delta}^{\mathrm{T}}, \boldsymbol{g}_{\Delta}^{\mathrm{T}}, \boldsymbol{0}_{J-\Delta-L}^{\mathrm{T}}\right]^{\mathrm{T}}$$

corresponds to the desired shortened channel response (in the CP range). Thus

$$\boldsymbol{g}_{\Delta} = \left[g(\Delta), g(\Delta+1), \ \ldots, g(\Delta+L-1)\right]^{\mathrm{T}}$$

Let

$$g_{\Delta}(i) = g(\Delta + i)$$

Then, we have

$$\boldsymbol{g}_{\Delta} = \left[g_{\Delta}(0), g_{\Delta}(1), \ \ldots, g_{\Delta}(L-1)\right]^{\mathrm{T}}$$

The second part

$$\boldsymbol{g}_{\mathrm{I}} = \left[g(0), \ \ldots, g_{\Delta}(-1), \boldsymbol{0}_{L}^{\mathrm{T}}, g_{\Delta}(L), \ \ldots, g(J-1)\right]^{\mathrm{T}}$$

is the equivalent channel response outside the CP region.

We can express $\boldsymbol{g}_{\mathrm{S}}$ and $\boldsymbol{g}_{\mathrm{I}}$ in terms of the channel matrix $\boldsymbol{H}$ and the TEQ vector $\boldsymbol{w}$ as $\boldsymbol{g}_{\mathrm{S}} = \boldsymbol{D}_{\mathrm{S}}\boldsymbol{H}\boldsymbol{w}$ and $\boldsymbol{g}_{\mathrm{I}} = \boldsymbol{D}_{\mathrm{I}}\boldsymbol{H}\boldsymbol{w}$,

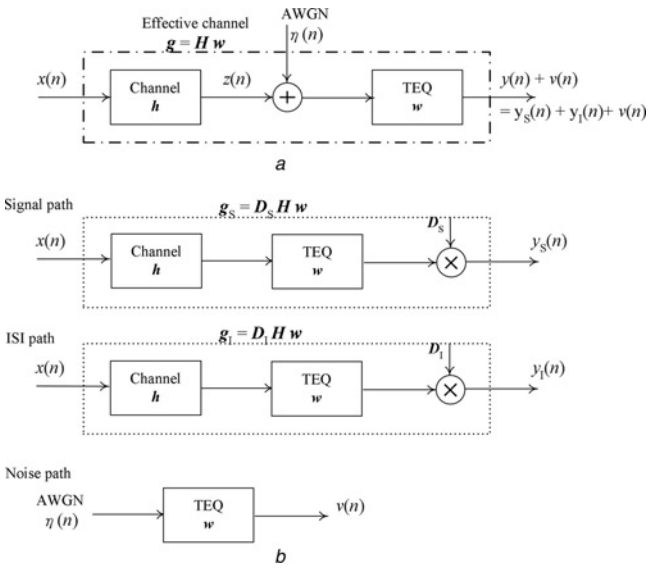

Figure 2 *Effective channel in a DMT system and its decomposition*

a Effective channel in a DMT system

b Decomposition of received signal: desired signal path, ISI path, and noise path ($\boldsymbol{H}$ is the channel matrix)

respectively, where

$$\boldsymbol{D}_{\mathrm{S}} = \mathrm{diag}\left[\boldsymbol{0}_{\Delta}^{\mathrm{T}}, \boldsymbol{1}_{L}^{\mathrm{T}}, \boldsymbol{0}_{J-\Delta-L}^{\mathrm{T}}\right]$$

$$\boldsymbol{D}_{\mathrm{I}} = \boldsymbol{I}_{J} - \boldsymbol{D}_{\mathrm{S}} = \mathrm{diag}\left[\boldsymbol{1}_{\Delta}^{\mathrm{T}}, \boldsymbol{0}_{L}^{\mathrm{T}}, \boldsymbol{1}_{J-\Delta-L}^{\mathrm{T}}\right]$$

and

$$\boldsymbol{H} = \begin{bmatrix} h(0) & 0 & \ldots & 0 \\ h(1) & h(0) & \ldots & 0 \\ \vdots & \vdots & \ddots & \vdots \\ h(I-1) & h(I-2) & \ldots & h(I-N) \\ 0 & h(I-1) & \ldots & h(I-N+1) \\ \vdots & \vdots & \ddots & \vdots \\ 0 & 0 & \ldots & h(I-1) \end{bmatrix}_{J\times N}.$$

Define an $M \times J$ matrix $\boldsymbol{T}_{\mathrm{G}}$ such that when $\boldsymbol{g}_{\mathrm{I}}$ and $\boldsymbol{g}_{\mathrm{S}}$ are multiplied by $\boldsymbol{T}_{\mathrm{G}}$, they will be shifted with the optimal delay Δ, and then padded with zeros to have a size of M. That is,

$$\boldsymbol{T}_{\mathrm{G}} = \begin{bmatrix} \boldsymbol{0}_{(J-\Delta)\times\Delta} & \boldsymbol{I}_{J-\Delta} \\ \boldsymbol{I}_{\Delta} & \boldsymbol{0}_{\Delta\times(J-\Delta)} \\ & \boldsymbol{0}_{(M-J)\times J} \end{bmatrix}_{M\times J}$$

Additionally, let $\tilde{\boldsymbol{g}}_{\mathrm{S}}, \tilde{\boldsymbol{g}}_{\mathrm{I}}$ be the DFT of $\boldsymbol{g}_{\mathrm{S}}$, and $\boldsymbol{g}_{\mathrm{I}}$, respectively. Thus, we have

$$\tilde{\boldsymbol{g}}_{\mathrm{S}} = [\tilde{g}_{\mathrm{S}}(0), \ldots, \tilde{g}_{\mathrm{S}}(M-1)]^{\mathrm{T}} = \boldsymbol{F}\boldsymbol{T}_{\mathrm{G}}\boldsymbol{g}_{\mathrm{S}}$$

and

$$\tilde{\boldsymbol{g}}_{\mathrm{I}} = \left[\tilde{g}_{\mathrm{I}}(0), \ldots, \tilde{g}_{\mathrm{I}}(M-1)\right]^{\mathrm{T}} = \boldsymbol{F}\boldsymbol{T}_{\mathrm{G}}\boldsymbol{g}_{\mathrm{I}}$$

where $\tilde{g}_{\mathrm{S}}(k) = \boldsymbol{f}^{\mathrm{T}}(k)\boldsymbol{T}_{\mathrm{G}}\boldsymbol{D}_{\mathrm{S}}\boldsymbol{H}\boldsymbol{w}$ and $\tilde{g}_{\mathrm{I}}(k) = \boldsymbol{f}^{\mathrm{T}}(k)\boldsymbol{T}_{\mathrm{G}}\boldsymbol{D}_{\mathrm{I}}\boldsymbol{H}\boldsymbol{w}$ are the $(k+1)$th elements of $\tilde{\boldsymbol{g}}_{\mathrm{S}}$, and $\tilde{\boldsymbol{g}}_{\mathrm{I}}$, respectively. We can express $\boldsymbol{g}_{\mathrm{S}}$ and $\boldsymbol{g}_{\mathrm{I}}$ as

$$\begin{cases} \boldsymbol{g}_{\mathrm{S}} = [g_{\mathrm{S}}(0), \ldots, g_{\mathrm{S}}(J-1)]^{\mathrm{T}} \text{ and} \\ \boldsymbol{g}_{\mathrm{I}} = [g_{\mathrm{I}}(0), \ldots, g_{\mathrm{I}}(J-1)]^{\mathrm{T}} \end{cases}$$

respectively, where $g_{\mathrm{S}}(l)$, $g_{\mathrm{I}}(l)$ are the $(l+1)$th elements of $\boldsymbol{g}_{\mathrm{S}}$, and $\boldsymbol{g}_{\mathrm{I}}$, respectively. Let $y_{\mathrm{S}}(n)$ and $y_{\mathrm{I}}(n)$ be the desired and residual ISI components of $y(n)$, respectively. Thus we have

$$y(n) = y_{\mathrm{S}}(n) + y_{\mathrm{I}}(n)$$

where $y_{\mathrm{S}}(n) = x(n) * g_{\mathrm{S}}(n)$, and $y_{\mathrm{I}}(n) = x(n) * g_{\mathrm{I}}(n)$. Consequently, we can also decompose $\boldsymbol{y}_i$ as

$$\boldsymbol{y}_i = \boldsymbol{y}_{S,i} + \boldsymbol{y}_{I,i} \tag{1}$$

where

$$\boldsymbol{y}_{\mathrm{S},i} = [y_{\mathrm{S}}(iK+\Delta+L), \ldots, y_{\mathrm{S}}(iK+\Delta+K-1)]^{\mathrm{T}} \text{ and}$$
$$\boldsymbol{y}_{\mathrm{I},i} = [y_{\mathrm{I}}(iK+\Delta+L), \ldots, y_{\mathrm{I}}(iK+\Delta+K-1)]^{\mathrm{T}}$$

Moreover, let

$$\tilde{\boldsymbol{y}}_{\mathrm{S},i} = [\tilde{y}_{\mathrm{S},i}(0), \ldots, \tilde{y}_{\mathrm{S},i}(M-1)]^{\mathrm{T}}$$
$$\tilde{\boldsymbol{y}}_{\mathrm{I},i} = [\tilde{y}_{\mathrm{I},i}(0), \ldots, \tilde{y}_{\mathrm{I},i}(M-1)]^{\mathrm{T}}$$

be the M-DFT of $\boldsymbol{y}_{\mathrm{S},i}$, and $\boldsymbol{y}_{\mathrm{I},i}$, respectively. Then, $\tilde{\boldsymbol{y}}_{\mathrm{S},i} = \boldsymbol{F}\boldsymbol{y}_{\mathrm{S},i}$, $\tilde{\boldsymbol{y}}_{\mathrm{I},i} = \boldsymbol{F}\boldsymbol{y}_{\mathrm{I},i}$, and $\tilde{\boldsymbol{y}}_i$ can be rewritten as $\tilde{\boldsymbol{y}}_i = \tilde{\boldsymbol{y}}_{\mathrm{S},i} + \tilde{\boldsymbol{y}}_{\mathrm{I},i}$. Fig. 2*b* shows the decomposition of $y(n) + \eta(n)$ in Fig. 2*a* into $y_{\mathrm{S}}(n)$, $y_{\mathrm{I}}(n)$, and $\eta(n)$, respectively.

2.2 Conventional TEQ design

Let $s_{\mathrm{d}}(k)$ be the signal power in the $(k+1)$th subchannel and

$$s_{\mathrm{d}}(k) = \mathrm{E}\{|\tilde{d}_i(k)|^2\}$$

where $\mathrm{E}\{\cdot\}$ is the expectation operation. Also, let $s_\eta(k)$ be the corresponding noise power, and

$$s_\eta(k) = \mathrm{E}\{|\tilde{\eta}_i(k)|^2\}$$

It is generally assumed that the transmit data are white, and hence the power is identical for each subchannel; that is $s_{\mathrm{d}}(k) = s_{\mathrm{d}}$, where s_{d} is a constant. Similarly, the subchannel noise power $s_\eta(k) = s_\eta$, where s_η is a constant. From the definitions shown above, it is straightforward to have

$$\mathrm{E}\{|\tilde{y}_{S,i}(k)|^2\} = s_{\mathrm{d}}|\tilde{g}_{\mathrm{S}}(k)|^2,\ \mathrm{E}\{|\tilde{y}_{I,i}(k)|^2\} = s_{\mathrm{d}}|\tilde{g}_{\mathrm{I}}(k)|^2 \quad \text{and}$$
$$\mathrm{E}\{|\tilde{v}_i(k)|^2\} = s_\eta|\tilde{w}(k)|^2$$

where

$$\tilde{w}(k) = \boldsymbol{f}^{\mathrm{T}}(k)\boldsymbol{T}_W\boldsymbol{w}$$

Here

$$\tilde{\boldsymbol{w}} = [\tilde{w}(0), \ldots, \tilde{w}(M-1)]^{\mathrm{T}}$$

is the M-DFT of $\boldsymbol{w}$, and $\boldsymbol{T}_W$ is an $M \times N$ matrix padding zeros in $\boldsymbol{w}$ to a size of M, i.e.

$$\boldsymbol{T}_W = [\boldsymbol{I}_N, \boldsymbol{0}_{(M-N)\times N}]^{\mathrm{T}}$$

The subchannel signal-to-interference plus noise ratio (SINR) at the DFT output is then

$$\mathrm{SINR}(k) = \frac{\mathrm{E}\left\{\left|\tilde{y}_{\mathrm{S},i}(k)\right|^2\right\}}{\mathrm{E}\left\{\left|\tilde{v}_i(k)\right|^2\right\} + \mathrm{E}\left\{\left|\tilde{y}_{\mathrm{I},i}(k)\right|^2\right\}} = \frac{s_{\mathrm{d}}\left|\tilde{g}_{\mathrm{S}}(k)\right|^2}{s_\eta|\tilde{w}(k)|^2 + s_{\mathrm{d}}\left|\tilde{g}_{\mathrm{I}}(k)\right|^2} \tag{2}$$

After some mathematical manipulations, the subchannel SINR can be rewritten as

$$\mathrm{SINR}(k) = \frac{s_{\mathrm{d}}(k)\left|\boldsymbol{f}^{\mathrm{T}}(k)\boldsymbol{T}_{\mathrm{G}}\boldsymbol{D}_{\mathrm{S}}\boldsymbol{H}\boldsymbol{w}\right|^2}{s_\eta(k)\left|\boldsymbol{f}^{\mathrm{T}}(k)\boldsymbol{T}_W\boldsymbol{w}\right|^2 + s_{\mathrm{d}}(k)\left|\boldsymbol{f}^{\mathrm{T}}(k)\boldsymbol{T}_{\mathrm{G}}\boldsymbol{D}_{\mathrm{I}}\boldsymbol{H}\boldsymbol{w}\right|^2} = \frac{\boldsymbol{w}^{\mathrm{T}}\boldsymbol{A}(k)\boldsymbol{w}}{\boldsymbol{w}^{\mathrm{T}}\boldsymbol{B}(k)\boldsymbol{w}} \tag{3}$$

where

$$\boldsymbol{A}(k) = s_{\mathrm{d}}(k)\boldsymbol{H}^{\mathrm{T}}\boldsymbol{D}_{\mathrm{S}}^{\mathrm{T}}\boldsymbol{T}_{\mathrm{G}}^{\mathrm{T}}\boldsymbol{f}^*(k)\boldsymbol{f}^{\mathrm{T}}(k)\boldsymbol{T}_{\mathrm{G}}\boldsymbol{D}_{\mathrm{S}}\boldsymbol{H}, \text{ and}$$
$$\boldsymbol{B}(k) = s_\eta(k)\boldsymbol{T}_W^{\mathrm{T}}\boldsymbol{f}^*(k)\boldsymbol{f}^{\mathrm{T}}(k)\boldsymbol{T}_W + s_{\mathrm{d}}(k)\boldsymbol{H}^{\mathrm{T}}\boldsymbol{D}_{\mathrm{I}}^{\mathrm{T}}\boldsymbol{T}_{\mathrm{G}}^{\mathrm{T}}\boldsymbol{f}^*(k) \times \boldsymbol{f}^{\mathrm{T}}(k)\boldsymbol{T}_{\mathrm{G}}\boldsymbol{D}_{\mathrm{I}}\boldsymbol{H}$$

Using the result above, we can express the capacity for a DMT system as

$$B = \sum_{k\in\Omega}\log_2\left(1 + \frac{1}{\Gamma}\frac{\boldsymbol{w}^{\mathrm{T}}\boldsymbol{A}(k)\boldsymbol{w}}{\boldsymbol{w}^{\mathrm{T}}\boldsymbol{B}(k)\boldsymbol{w}}\right)\text{bits per symbol} \tag{4}$$

where Ω is the set of total usable subchannels, namely,

$$\Omega = \{0, 1, \ldots, (M/2)-1\}$$

and Γ the SNR gap [12]. Thus, we can obtain the optimum TEQ vector $\boldsymbol{w}$ with the maximisation of (4). This method is called MBR [12]. Note that (4) is a non-linear function of $\boldsymbol{w}$; it can only be solved by some non-linear optimisation methods, such as the quasi-Newton or simplex algorithms. As the non-linear optimisation method often requires extensive computations, a suboptimal method, min-ISI, was then developed [12]. It was shown that the performance of min-ISI can effectively approach the performance of MBR.

2.3 Conventional SINR calculation

As discussed in the previous section, interference in a subchannel consists of noise and residual ISI. Let

$$\boldsymbol{x}_i = [x(iK+L), \ldots, x(iK+K-1)]^{\mathrm{T}}$$

doi: 10.1049/iet-com.2008.0133

be the ith data symbol at the DMT transmitter output. As $\boldsymbol{x}_i$ contains a CP, the desired signal component in (1) can be expressed as

$$\boldsymbol{y}_{\mathrm{S},i} = \boldsymbol{x}_i \circledast \boldsymbol{g}$$

Here, we extend the circular convolution operation to vectors for notational simplicity. With the M-DFT operation

$$\tilde{\boldsymbol{y}}_{\mathrm{S},i} = \tilde{\boldsymbol{x}}_i \bullet \tilde{\boldsymbol{g}}$$

Note that noise does not contain CPs; thus, $\boldsymbol{v}_i \neq \boldsymbol{\eta}_i \circledast \boldsymbol{w}$, and $\tilde{\boldsymbol{v}}_i \neq \tilde{\boldsymbol{\eta}}_i \bullet \tilde{\boldsymbol{w}}$. As a result

$$\mathrm{E}\{|\tilde{v}_i(k)|^2\} \neq s_\eta |\tilde{w}(k)|^2$$

Also, the residual ISI response is the ISI response outside the CP region. The corresponding residual ISI cannot be obtained from the circular convolution of the input signal and $\boldsymbol{g}_{\mathrm{I}}$. Thus

$$\mathrm{E}\{|\tilde{y}_{\mathrm{I},i}(k)|^2\} \neq s_{\mathrm{d}} |\tilde{g}_{\mathrm{I}}(k)|^2$$

From these facts, we conclude that SINR calculated with (2) is not correct. In other words

$$\mathrm{SINR}(k) \neq \frac{s_{\mathrm{d}} |\tilde{g}_{\mathrm{S}}(k)|^2}{s_\eta |\tilde{w}(k)|^2 + s_{\mathrm{d}} |\tilde{g}_{\mathrm{I}}(k)|^2} \tag{5}$$

Although the properties analysed above are simple, they were not discovered until recently [21]. It was also independently observed in [20]. As the SINR is erroneously calculated, the optimum solution obtained with (4) is no longer optimal. In the following section, we will analyse the effect of the non-cyclic noise and residual ISI, and derive correct formulae for their power calculations.

3 Analysis of noise/residual ISI effect

3.1 Analysis of noise effect

Let

$$\boldsymbol{s}_{\mathrm{d}} = [s_{\mathrm{d}}(0), s_{\mathrm{d}}(1), \ldots, s_{\mathrm{d}}(M-1)]^{\mathrm{T}} = s_{\mathrm{d}} \cdot \mathbf{1}_M \quad \text{and}$$
$$\boldsymbol{s}_\eta = [s_{\mathrm{d}}(\eta), s_\eta(1), \ldots, s_\eta(M-1)]^{\mathrm{T}} = s_\eta \cdot \mathbf{1}_M$$

where

$$s_{\mathrm{d}} = M \cdot \mathrm{E}\{x^2(n)\} = M\sigma_{\mathrm{d}}^2 \quad \text{and}$$
$$s_\eta = M \cdot \mathrm{E}\{\eta^2(n)\} = M\sigma_\eta^2$$

Recall $\boldsymbol{g}_\Delta$ defined in Section 2.1, and define $\boldsymbol{G}_\Delta$ as an $M \times M$ circular channel matrix

$$\boldsymbol{G}_\Delta = \begin{bmatrix} g_\Delta(0) & 0 & \ldots & 0 & g_\Delta(L-1) & \ldots & g_\Delta(2) & g_\Delta(1) \\ g_\Delta(1) & g_\Delta(0) & \ldots & 0 & 0 & \ldots & g_\Delta(3) & g_\Delta(2) \\ \vdots & \vdots & \ddots & \ddots & \ddots & \ddots & \ddots & \vdots \\ 0 & 0 & \ldots & g_\Delta(L-2) & g_\Delta(L-3) & \ldots & g_\Delta(0) & 0 \\ 0 & 0 & \ldots & g_\Delta(L-1) & g_\Delta(L-2) & \ldots & g_\Delta(1) & g_\Delta(0) \end{bmatrix} \tag{6}$$

We first consider a scenario in which $\boldsymbol{g}$ does not have residual ISI. The DFT output of the received symbol $\tilde{\boldsymbol{y}}_i = \tilde{\boldsymbol{y}}_{S,i}$ can be written as

$$\tilde{\boldsymbol{y}}_{\mathrm{S},i} = \boldsymbol{F}\boldsymbol{y}_{\mathrm{S},i} = \boldsymbol{F}\boldsymbol{G}_\Delta \boldsymbol{x}_i = \tilde{\boldsymbol{G}}_\Delta \boldsymbol{x}_i$$

where $\tilde{\boldsymbol{G}}_\Delta = \boldsymbol{F}\boldsymbol{G}_\Delta$. Define the vector consisting of the subchannel received signal powers as $\boldsymbol{s}_y$. Then

$$\boldsymbol{s}_y = \mathrm{E}\left\{\langle \tilde{\boldsymbol{y}}_{\mathrm{S},i} \rangle^2\right\}$$

It follows that

$$\mathrm{E}\left\{\langle \tilde{\boldsymbol{y}}_{\mathrm{S},i} \rangle^2\right\} = \langle \mathrm{E}\{\tilde{\boldsymbol{G}}_\Delta \boldsymbol{x}_i\} \rangle^2 = \sigma_{\mathrm{d}}^2 \langle \tilde{\boldsymbol{G}}_\Delta \rangle^2$$

Let

$$\boldsymbol{G}_\Delta = [\boldsymbol{\rho}(0), \ldots, \boldsymbol{\rho}(M-1)]$$

where $\boldsymbol{\rho}(l)$ is the $(l+1)$th column of $\boldsymbol{G}_\Delta$. Then

$$\tilde{\boldsymbol{G}}_\Delta = [\tilde{\boldsymbol{\rho}}(0), \ldots, \tilde{\boldsymbol{\rho}}(M-1)]$$

where $\tilde{\boldsymbol{\rho}}(k) = \boldsymbol{F}\boldsymbol{\rho}(k)$ is the $(k+1)$th column vector of $\tilde{\boldsymbol{G}}_\Delta$. Thus

$$\boldsymbol{s}_y = \mathrm{E}\left\{\langle \tilde{\boldsymbol{y}}_{\mathrm{S},i} \rangle^2\right\} = \sigma_{\mathrm{d}}^2 \sum_{k=0}^{M-1} \langle \tilde{\boldsymbol{\rho}}(k) \rangle^2 \tag{7}$$

From (6), we find that each $\boldsymbol{\rho}(k)$ in $\boldsymbol{s}_y$ contains a circular shift of the equivalent channel vector $\boldsymbol{g}_\Delta$. Thus

$$\langle \tilde{\boldsymbol{\rho}}(k) \rangle^2 = \langle \tilde{\boldsymbol{g}}_\Delta \rangle^2$$

for all k's, where

$$\tilde{\boldsymbol{g}}_\Delta = \boldsymbol{F}\boldsymbol{T}_\Delta \boldsymbol{g}_\Delta = \boldsymbol{F}\boldsymbol{\rho}(0)$$

and $\boldsymbol{T}_\Delta$ is an $M \times L$ zero padding matrix used to increase the size of $\boldsymbol{g}_\Delta$ to M. Consequently

$$\boldsymbol{s}_y = M\sigma_{\mathrm{d}}^2\langle\tilde{\boldsymbol{g}}_\Delta\rangle^2 = s_{\mathrm{d}}\langle\tilde{\boldsymbol{g}}_\Delta\rangle^2$$

for all k's.

Without loss of generality, we let the length of the TEQ, N, be smaller than the CP length, L. Furthermore, let

$$\boldsymbol{\eta}_{C,i} = [\eta(iK+\Delta), \eta(iK+\Delta+1), \ldots, \eta(iK+\Delta+L-1)]^{\mathrm{T}}$$

which is the noise sequence in the CP region of the ith symbol. Thus, the noise vector in the ith DMT symbol can be defined as

$$\check{\boldsymbol{\eta}}_i = \left[\boldsymbol{\eta}_{\mathrm{C},i}^{\mathrm{T}}, \boldsymbol{\eta}_i^{\mathrm{T}}\right]^{\mathrm{T}}$$

Then, we can denoted the TEQ-filtered noise vector as

$$\boldsymbol{v}_i = \boldsymbol{W}\check{\boldsymbol{\eta}}_i$$

where $\boldsymbol{W}$ is an $M \times K$ matrix composing of TEQ coefficients as

$$\boldsymbol{W} = \begin{bmatrix} 0 & \ldots & w(N-1) & w(N-2) & \ldots \\ 0 & \ldots & 0 & w(N-1) & \ldots \\ \vdots & \ddots & \vdots & \vdots & \ddots \\ 0 & \ldots & 0 & 0 & \ldots \\ 0 & \ldots & 0 & 0 & \ldots \end{bmatrix} \begin{bmatrix} 0 & \ldots & 0 & 0 \\ 0 & \ldots & 0 & 0 \\ \vdots & \ddots & \vdots & \vdots \\ w(N-1) & \ldots & w(0) & 0 \\ 0 & \ldots & w(1) & w(0) \end{bmatrix}_{M\times K} \tag{8}$$

Note that the first $(L-N)$ column vectors of $\boldsymbol{W}$ are zero vectors, $\boldsymbol{0}_M$. The DFT of the TEQ-filtered noise vector in the i symbol, denoted as $\tilde{\boldsymbol{v}}_i$, is then

$$\tilde{\boldsymbol{v}}_i = \boldsymbol{F}\boldsymbol{v}_i = \boldsymbol{F}\boldsymbol{W}\check{\boldsymbol{\eta}}_i = \tilde{\boldsymbol{W}}\check{\boldsymbol{\eta}}_i$$

where $\tilde{\boldsymbol{W}} = \boldsymbol{F}\boldsymbol{W}$ is the DFT of $\boldsymbol{W}$. Note that $\boldsymbol{W}$ is not a circular matrix like $\boldsymbol{G}_\Delta$, and $\boldsymbol{W}$ can be expressed in another form $[\boldsymbol{u}(0), \ldots, \boldsymbol{u}(K-1)]$, where $\boldsymbol{u}(p)$ is

$$\boldsymbol{u}(p) = \begin{cases} \boldsymbol{0}_M & \text{if } 0 \le p \le L-N \\ \left[w(L-p), \ldots, w(N-1), \boldsymbol{0}_{K-N-p}^{\mathrm{T}}\right]^{\mathrm{T}} & \text{if } L-N+1 \le p \le L-1 \\ \left[\boldsymbol{0}_{p-L}^{\mathrm{T}}, \boldsymbol{w}^{\mathrm{T}}, \boldsymbol{0}_{K-N-p}^{\mathrm{T}}\right]^{\mathrm{T}} & \text{if } L \le p \le K-N \\ \left[\boldsymbol{0}_{p-L}^{\mathrm{T}}, w(0), w(1), \ldots, w(K-1-p)\right]^{\mathrm{T}} & \text{if } K-N+1 \le p \le K-1 \end{cases} \tag{9}$$

Let $\boldsymbol{s}_v$ denote the vector containing the power of TEQ-filtered noise in subchannels. Thus

$$\boldsymbol{s}_v = \mathrm{E}\{\langle\tilde{\boldsymbol{v}}_i\rangle^2\} = \mathrm{E}\{\langle\tilde{\boldsymbol{W}}\check{\boldsymbol{\eta}}_i\rangle^2\} = \sigma_\eta^2\langle\tilde{\boldsymbol{W}}\rangle^2 = \sigma_\eta^2\sum_{p=0}^{K-1}\langle\tilde{\boldsymbol{u}}(p)\rangle^2 \tag{10}$$

where $\tilde{\boldsymbol{u}}(p) = \boldsymbol{F}\boldsymbol{u}(p)$ is the DFT of $\boldsymbol{u}(p)$, and

$$\mathrm{E}\{\langle\check{\boldsymbol{\eta}}_i\rangle^2\} = \sigma_\eta^2 \cdot \boldsymbol{1}_K$$

For simplicity, we let $\boldsymbol{W}_1$ be the matrix formed by $\boldsymbol{u}(p)$ for $L-N+1 \le p \le L-1$, $\boldsymbol{W}_2$ be formed by $\boldsymbol{u}(p)$ for $L \le p \le K-N$, and $\boldsymbol{W}_3$ be formed by $\boldsymbol{u}(p)$ for $K-N+1 \le p \le K-1$, respectively. Then, we can rewrite $\boldsymbol{W}$ as

$$\boldsymbol{W} = \left[\boldsymbol{0}_{M\times(L-N)}, \boldsymbol{W}_1, \boldsymbol{W}_2, \boldsymbol{W}_3\right] \tag{11}$$

From (9), note that column vectors in $\boldsymbol{W}_2$ contain the complete TEQ vector $\boldsymbol{w}$, which implies that

$$\langle\tilde{\boldsymbol{u}}(p)\rangle^2 = \langle\tilde{\boldsymbol{w}}\rangle^2$$

for $L \le p \le K-N$. Each column vector in $\boldsymbol{W}_1$ and $\boldsymbol{W}_3$, however, contains only partial $\boldsymbol{w}$. As a result, $\boldsymbol{s}_v$ can be expressed as

$$\boldsymbol{s}_v = \sigma_\eta^2\left(\sum_{p=L-N+1}^{L-1}\langle\tilde{\boldsymbol{u}}(p)\rangle^2 + (M-N+1)\langle\tilde{\boldsymbol{w}}\rangle^2 + \sum_{p=K-N+1}^{K-1}\langle\tilde{\boldsymbol{u}}(p)\rangle^2\right) \tag{12}$$

Equation (12) gives the exact calculation of the noise power after TEQ. From (8), we can see that if the channel noise is cyclic, $\boldsymbol{W}$ can be folded to become an $M \times M$ circular matrix. In this case, we have

$$\boldsymbol{s}_v = M\sigma_\eta^2\langle\tilde{\boldsymbol{w}}\rangle^2 = s_\eta\langle\tilde{\boldsymbol{w}}\rangle^2 \tag{13}$$

doi: 10.1049/iet-com.2008.0133

Conventional SINR calculation, as shown in (2), uses (13). However, the channel noise is not cyclic; (13) is incorrect. From (12), we can clearly see that two more terms are induced because of the non-cyclic noise problem.

Now, we use some experimental results to show the differences between (12) and (13). The experiment settings are the standard ADSL environments [5], and will be described later in detail in Section 5. These experiments are all obtained with the standard test loop CSA #5, and the vector of the TEQ coefficients $\boldsymbol{w}$ is obtained with the min-ISI method [12]. As we can see from (13), $\boldsymbol{s}_v$, representing the TEQ-filtered noise spectrum, is equal to the multiplication of $\boldsymbol{s}_\eta$ and $\langle\tilde{\boldsymbol{w}}\rangle^2$. Thus, if the TEQ induces a null in its spectrum, it will also do that in $\boldsymbol{s}_v$. However, it is not the case in (12). Fig. 3 shows the contribution of $\boldsymbol{W}_1$, $\boldsymbol{W}_2$, and $\boldsymbol{W}_3$, to $\boldsymbol{s}_v$, respectively. Only $\boldsymbol{W}_2$ shows the same spectrum characteristic as that of $\boldsymbol{w}$. As mentioned previously, column vectors of both $\boldsymbol{W}_1$ and $\boldsymbol{W}_3$ contain only partial $\boldsymbol{w}$, and their spectrum characteristics are different from those of $\boldsymbol{w}$. As we can see from the figure, spectrum nulls introduced by the TEQ disappeared in spectrums yielded by $\boldsymbol{W}_1$ and $\boldsymbol{W}_3$. Fig. 4 shows the TEQ-filtered noise spectrums calculated with (12) and (13), and Fig. 5 shows the zoomed spectrum around nulls. The simulated noise power is also shown in the figures, which are obtained with 500 DMT symbols. It is apparent that the magnitudes at TEQ-induced nulls increase in the spectrum calculated with (12), and it is accurate. We then conclude that noise power tends to be higher in the spectrum with (12). This will have a great impact on the signal-to-noise ratio (SNR) at spectrum nulls induced by the TEQ.

3.2 Analysis of residual ISI

In general, a TEQ cannot be designed to shorten the channel into the CP range completely. The resultant channel

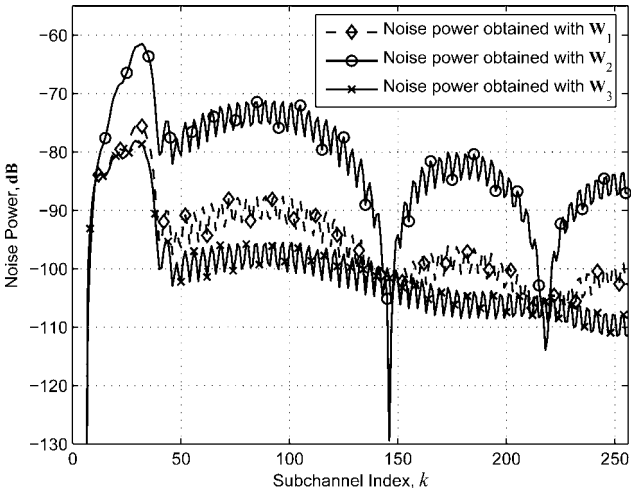

Figure 3 *Decomposed TEQ-filtered noise powers (N = 16, CSA#5 Loop)*

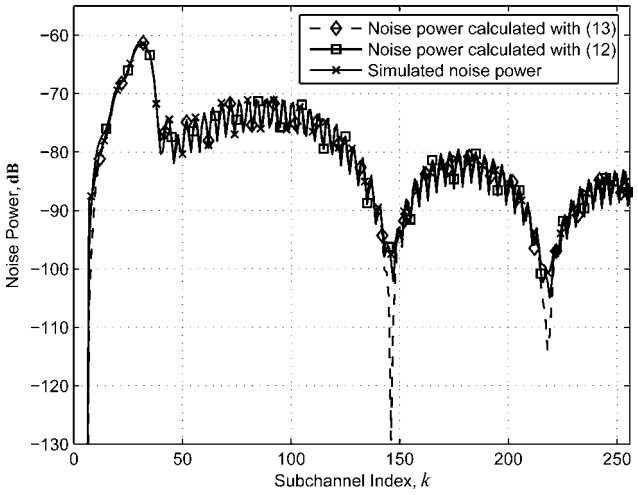

Figure 4 *Comparison of TEQ-filtered noise powers; power calculated with (13), power calculated with (12) (correct one), and simulated power (N = 16, CSA#5 Loop)*

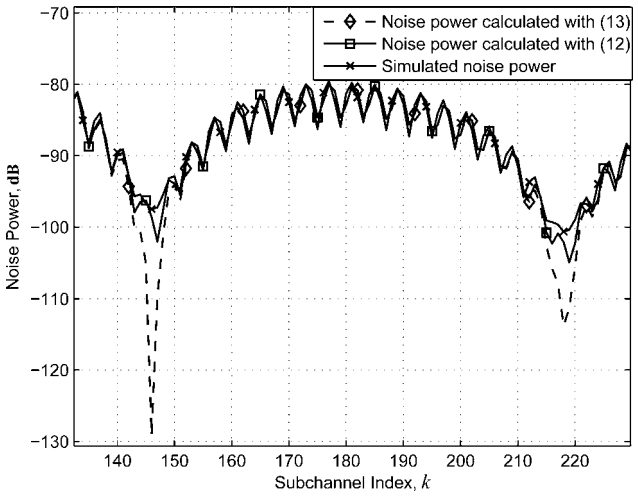

Figure 5 *A zoomed view of Fig. 4*

response outside the CP range consists of the residual ISI. Let the transmit signal in the CP range of the ith DMT symbol be

$$\boldsymbol{x}_{\mathrm{C},i} = [x(iK), x(iK+1), \ldots, x(iK+L-1)]^{\mathrm{T}}$$

We then have the complete ith DMT symbol

$$\check{\boldsymbol{x}}_i = \left[\boldsymbol{x}_{\mathrm{C},i}^{\mathrm{T}}, \boldsymbol{x}_i^{\mathrm{T}}\right]^{\mathrm{T}}$$

which is a $K \times 1$ column vector. Because of the delay Δ, the ith received DMT symbol $\check{\boldsymbol{x}}_i$ receives interference from $\check{\boldsymbol{x}}_{i-1}$ and $\check{\boldsymbol{x}}_{i+1}$. Define an extended symbol as

$$\check{\boldsymbol{x}}_{3,i} = [\check{\boldsymbol{x}}_{i-1}^{\mathrm{T}}, \check{\boldsymbol{x}}_i^{\mathrm{T}}, \check{\boldsymbol{x}}_{i+1}^{\mathrm{T}}]^{\mathrm{T}}$$

and the response of $\boldsymbol{g}_{\mathrm{I}}$ can be ignored when it exceeds M; that is

$$\boldsymbol{g}_{\mathrm{I}} = [g(0), \ldots, g_{\Delta}(-1), \mathbf{0}_L^{\mathrm{T}}, g_{\Delta}(L), \ldots, g(M-1)]^{\mathrm{T}}$$

which can be expressed in another form as

$$\boldsymbol{g}_{\mathrm{I}} = [g_{\mathrm{I}}(0), \ \ldots, g_{\mathrm{I}}(\Delta), g_{\mathrm{I}}(\Delta+1), \ldots, g_{\mathrm{I}}(M-1)]^{\mathrm{T}}$$

Thus, the power of $\check{\boldsymbol{x}}_{3,i}$ is

$$\mathrm{E}\{\lfloor \check{\boldsymbol{x}}_{3,i} \rceil^2\} = \sigma_{\mathrm{d}}^2 \cdot \begin{bmatrix} \boldsymbol{C}_{\mathrm{S}} & \mathbf{0}_{K\times K} & \mathbf{0}_{K\times K} \\ \mathbf{0}_{K\times K} & \boldsymbol{C}_{\mathrm{S}} & \mathbf{0}_{K\times K} \\ \mathbf{0}_{K\times K} & \mathbf{0}_{K\times K} & \boldsymbol{C}_{\mathrm{S}} \end{bmatrix}$$

where

$$\boldsymbol{C}_{\mathrm{S}} = \boldsymbol{I}_{K\times K} + \begin{bmatrix} \mathbf{0}_{L\times M} & \boldsymbol{I}_{L\times L} \\ \mathbf{0}_{M\times M} & \mathbf{0}_{M\times L} \end{bmatrix}$$

Using vector representation, we can express the residual ISI $\boldsymbol{y}_{\mathrm{I},i}$ in (1) as

$$\boldsymbol{y}_{\mathrm{I},i} = \boldsymbol{C}_{\mathrm{I}} \check{\boldsymbol{x}}_{3,i}$$

where

$$\boldsymbol{C}_{\mathrm{I}} = \left[\boldsymbol{c}_{\mathrm{I}}(0), \ldots, \boldsymbol{c}_{\mathrm{I}}(3K-1)\right]$$

is the matrix with residual ISI coefficients. We have the following decomposition

$$\boldsymbol{C}_{\mathrm{I}} = \left[\mathbf{0}_{M\times(2L+\Delta+1)}, \boldsymbol{C}_1, \boldsymbol{C}_2, \boldsymbol{C}_3, \mathbf{0}_{M\times(K-\Delta)}\right]_{M\times 3K}$$

where

$$\boldsymbol{C}_1 = \begin{bmatrix} g_{\mathrm{I}}(M-1) & \ldots & g_{\mathrm{I}}(1) \\ 0 & \ldots & g_{\mathrm{I}}(2) \\ \vdots & \ddots & \vdots \\ 0 & \ldots & g_{\mathrm{I}}(M-1) \\ 0 & \ldots & 0 \end{bmatrix}_{M\times(M-1)}$$

$$\boldsymbol{C}_2 = \begin{bmatrix} g_{\mathrm{I}}(0) & g_{\mathrm{I}}(1) & \ldots & g_{\mathrm{I}}(M-1) \end{bmatrix}_{M\times 1}^{\mathrm{T}} \qquad (14)$$

$$\boldsymbol{C}_3 = \begin{bmatrix} 0 & \ldots & 0 & 0 \\ g_{\mathrm{I}}(0) & \ldots & 0 & 0 \\ \vdots & \ddots & \vdots & \vdots \\ g_{\mathrm{I}}(M-2) & \ldots & g_{\mathrm{I}}(1) & g_{\mathrm{I}}(0) \end{bmatrix}_{M\times(M-1)}$$

Let

$$\begin{aligned} \tilde{\boldsymbol{C}}_{\mathrm{I}} &= \boldsymbol{F}\boldsymbol{C}_{\mathrm{I}} \\ &= \left[\mathbf{0}_{M\times(2L+\Delta+1)}, \tilde{\boldsymbol{c}}_{\mathrm{I}}(1), \ldots, \tilde{\boldsymbol{c}}_{\mathrm{I}}(2M-1), \mathbf{0}_{M\times(K-\Delta)}\right] \end{aligned}$$

be the DFT of $\boldsymbol{C}_{\mathrm{I}}$, where

$$\tilde{\boldsymbol{c}}_{\mathrm{I}}(p) = \boldsymbol{F}\boldsymbol{c}_{\mathrm{I}}(2L+\Delta+p), \ \text{for } 1 \le p \le 2M-1$$

At the DFT output, we have the residual ISI component of the received signal

$$\tilde{\boldsymbol{y}}_{\mathrm{I},i} = \boldsymbol{F}\boldsymbol{y}_{\mathrm{I},i} = \boldsymbol{F}\boldsymbol{C}_{\mathrm{I}}\check{\boldsymbol{x}}_{3,i} = \tilde{\boldsymbol{C}}_{\mathrm{I}}\check{\boldsymbol{x}}_{3,i}$$

Denote $\boldsymbol{s}_{\mathrm{I}}$ as the vector containing residual ISI power in subchannels. Then

$$\begin{aligned} \boldsymbol{s}_{\mathrm{I}} &= \mathrm{E}\left\{\langle \tilde{\boldsymbol{y}}_{\mathrm{I},i}\rangle^2\right\} = \mathrm{E}\left\{\langle \boldsymbol{F}\boldsymbol{C}_{\mathrm{I}}\check{\boldsymbol{x}}_{3,i}\rangle^2\right\} \\ &= \sigma_{\mathrm{d}}^2 \sum_{p=1}^{2M-1} \langle \tilde{\boldsymbol{c}}_{\mathrm{I}}(p)\rangle^2 + \sigma_{\mathrm{d}}^2 \sum_{p=M-L-\Delta}^{M-\Delta-1} \langle \tilde{\boldsymbol{c}}_{\mathrm{I}}(p)\rangle^2 \\ &\quad + \sigma_{\mathrm{d}}^2 \sum_{p=2M-\Delta}^{2M+L-\Delta-1} \langle \tilde{\boldsymbol{c}}_{\mathrm{I}}(p)\rangle^2 \end{aligned} \qquad (15)$$

where the last two terms in (15) are the interference power induced from the off-diagonal terms of $\mathrm{E}\{\lfloor \check{\boldsymbol{x}}_{3,i} \rceil^2\}$. Observe that only $\boldsymbol{C}_2$ has the complete residual ISI vector $\boldsymbol{g}_{\mathrm{I}}$. Thus

$$\langle \tilde{\boldsymbol{C}}_2\rangle^2 = \langle \tilde{\boldsymbol{g}}_{\mathrm{I}}\rangle^2$$

where

$$\tilde{\boldsymbol{C}}_2 = \boldsymbol{F}\boldsymbol{C}_2 = \tilde{\boldsymbol{c}}_{\mathrm{I}}(K+L)$$

Column vectors in $\boldsymbol{C}_1$ and $\boldsymbol{C}_3$ contain only partial $\boldsymbol{g}_{\mathrm{I}}$. If $\boldsymbol{g}_{\mathrm{I}}$ is in the CP range, then the circular convolution property can be applied. Then

$$\boldsymbol{s}_{\mathrm{I}} = M\sigma_{\mathrm{d}}^2\langle \tilde{\boldsymbol{g}}_{\mathrm{I}}\rangle^2 = s_d\langle \tilde{\boldsymbol{g}}_{\mathrm{I}}\rangle^2 \qquad (16)$$

This is the result used in (2). However, the residual ISI is the ISI outside the CP range, and (16) is not valid in practice.

Here, we also use some experimental results to show the difference between (15) and (16). The experiment settings are the same as those in Section 3.1. Fig. 6 shows the spectrums yielded by $\boldsymbol{C}_1$, $\boldsymbol{C}_2$, and $\boldsymbol{C}_3$ in (14), respectively. We can see that spectrums yielded by $\boldsymbol{C}_1$ and $\boldsymbol{C}_3$ are larger than that by $\boldsymbol{C}_2$, which is directly related to $\boldsymbol{g}_{\mathrm{I}}$. This phenomenon is more apparent in regions with spectrum nulls. Fig. 7 shows the spectrums obtained with (15) and (16), and Fig. 8 is a zoomed spectrum. The simulated ISI power is also shown in the figures, which are obtained with 500 DMT symbols. As revealed with the figures, the magnitudes at the nulls are significantly raised in the spectrum calculated with (15). Also, the spectrum agrees with that simulation very well. Similar to the case in Section 3.1, the SINR is reduced at spectrum nulls.

doi: 10.1049/iet-com.2008.0133

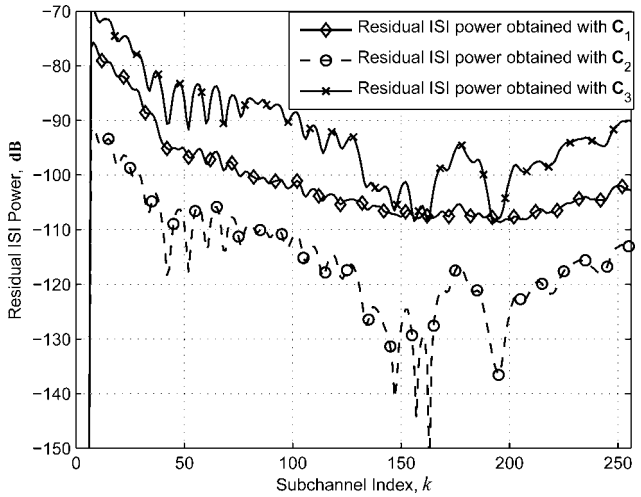

Figure 6 *Decomposed residual-ISI powers (N = 16, CSA#5 Loop)*

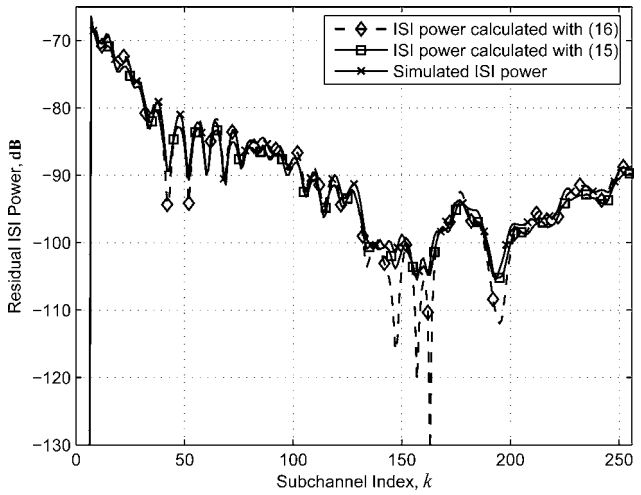

Figure 7 *Comparison of residual-ISI powers; power calculated with (16), power calculated with (15) (correct one), and simulated power (N = 16, CSA#5 Loop)*

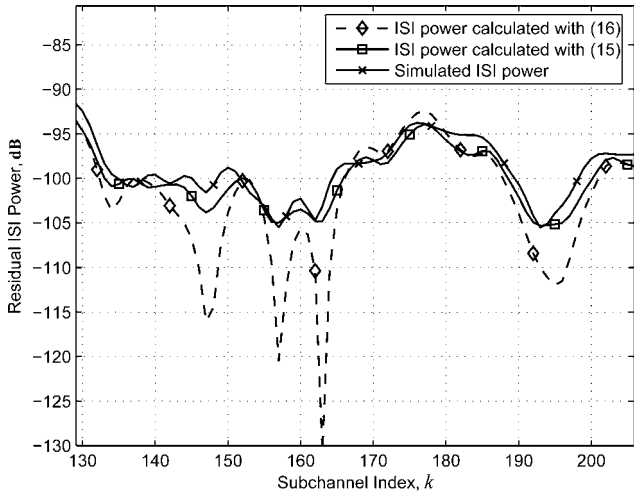

Figure 8 *A zoomed view of Fig. 7*

Combining the results in Section 3.1 and Section 3.2, we conclude that the SINR calculation in (3) is not correct. To have better loading performance, noise and residual ISI power should be revised to those in (12) and (15). In Section 4, we will use the corrected formula to propose a new TEQ scheme.

4 Proposed algorithm

The formulations in (12) and (15) is meant to demonstrate the effect of the non-cyclic property of noise and the residual ISI. To derive the optimum TEQ, we have to use another formulation. Rewrite the TEQ-filtered noise vector $\boldsymbol{v}_i$ as $\boldsymbol{v}_i = \boldsymbol{N}_i\boldsymbol{w}$, where $\boldsymbol{N}_i$ is a matrix with noise samples, i.e.

$$\boldsymbol{N}_i = \begin{bmatrix} \eta(iK+\Delta+L) & \dots & \eta(iK+\Delta+L-N+1) \\ \vdots & \ddots & \vdots \\ \eta(iK+\Delta+K-1) & \dots & \eta(iK+\Delta+K-N+1) \end{bmatrix}_{M\times N} \tag{17}$$

The DFT of the ith TEQ-filtered noise symbol at the $(k+1)$th subchannel is

$$\tilde{v}_i(k) = \boldsymbol{f}^{\mathrm{T}}(k)\boldsymbol{v}_i = \boldsymbol{f}^{\mathrm{T}}(k)\boldsymbol{N}_i\boldsymbol{w}$$

and the corresponding power is

$$\mathrm{E}\{|\tilde{v}_i(k)|^2\} = \mathrm{E}\left\{\left|\boldsymbol{f}^{\mathrm{T}}(k)\boldsymbol{N}_i\boldsymbol{w}\right|^2\right\} = \boldsymbol{w}^{\mathrm{T}}\boldsymbol{R}(k)\boldsymbol{w}$$

where

$$\boldsymbol{R}(k) = \mathrm{E}\{[\tilde{\boldsymbol{N}}_i^{\mathrm{T}}(k)]^2\}$$

and

$$\tilde{\boldsymbol{N}}_i(k) = \boldsymbol{f}^{\mathrm{T}}(k)\boldsymbol{N}_i$$

Similarly, we can rewrite the residual ISI, $\boldsymbol{y}_{\mathrm{I},i}$, in (1) as

$$\boldsymbol{y}_{\mathrm{I},i} = \boldsymbol{X}_i\boldsymbol{g}_{\mathrm{I}}$$

where

$$\boldsymbol{X}_i = \begin{bmatrix} x(iK+L-J+1) & \dots & x(iK+L) \\ \vdots & \ddots & \vdots \\ x(iK+K-J) & \dots & x(iK+K-1) \end{bmatrix}_{M\times J} \tag{18}$$

The DFT of the residual ISI at the $(k+1)$th subchannel is

$$\tilde{y}_{\mathrm{I},i}(k) = \boldsymbol{f}^{\mathrm{T}}(k)\boldsymbol{y}_{\mathrm{I},i} = \boldsymbol{f}^{\mathrm{T}}(k)\boldsymbol{X}_i\boldsymbol{D}_{\mathrm{I}}\boldsymbol{H}\boldsymbol{w}$$

and the corresponding power is

$$\mathrm{E}\{|\tilde{y}_{\mathrm{I},i}(k)|^2\} = \mathrm{E}\{|\boldsymbol{f}^{\mathrm{T}}(k)\boldsymbol{X}_i\boldsymbol{D}_{\mathrm{I}}\boldsymbol{H}\boldsymbol{w}|^2\} = \boldsymbol{w}^{\mathrm{T}}\boldsymbol{Q}(k)\boldsymbol{w}$$

where

$$\boldsymbol{Q}(k) = \boldsymbol{H}^{\mathrm{T}}\boldsymbol{D}_{\mathrm{I}}^{\mathrm{T}}\mathrm{E}\{\lfloor\tilde{\boldsymbol{X}}_i^{\mathrm{T}}(k)\rceil^2\}\boldsymbol{D}_{\mathrm{I}}\boldsymbol{H}$$

and

$$\tilde{\boldsymbol{X}}_i(k) = \boldsymbol{f}^{\mathrm{T}}(k)\boldsymbol{X}_i$$

Then, the subchannel SINR can be revised from (2) as

$$\mathrm{SINR}(k) = \frac{\mathrm{E}\{|\tilde{y}_{\mathrm{S},i}(k)|^2\}}{\mathrm{E}\{|\tilde{v}_i(k)|^2\} + \mathrm{E}\{|\tilde{y}_{\mathrm{I},i}(k)|^2\}} = \frac{\boldsymbol{w}^{\mathrm{T}}\boldsymbol{A}(k)\boldsymbol{w}}{\boldsymbol{w}^{\mathrm{T}}\boldsymbol{Y}(k)\boldsymbol{w}} \tag{19}$$

where $\boldsymbol{A}(k)$ is defined as that in (3), and

$$\boldsymbol{w}^{\mathrm{T}}\boldsymbol{Y}(k)\boldsymbol{w} = \boldsymbol{w}^{\mathrm{T}}[\boldsymbol{R}(k) + \boldsymbol{Q}(k)]\boldsymbol{w}$$

includes the noise power $\boldsymbol{w}^{\mathrm{T}}\boldsymbol{R}(k)\boldsymbol{w}$ and residual ISI power $\boldsymbol{w}^{\mathrm{T}}\boldsymbol{Q}(k)\boldsymbol{w}$. Finally, the capacity can be expressed in terms of the subchannel SINR (19) as

$$B = \sum_{k\in\Omega}\log_2\left(1 + \frac{1}{\Gamma}\frac{\boldsymbol{w}^{\mathrm{T}}\boldsymbol{A}(k)\boldsymbol{w}}{\boldsymbol{w}^{\mathrm{T}}\boldsymbol{Y}(k)\boldsymbol{w}}\right)\text{bits per symbol} \tag{20}$$

The optimum $\boldsymbol{w}$ can then be obtained by maximising B. To distinguish from the MBR method [12], we called the proposed method the enhanced MBR (EMBR) method.

The proposed EMBR method requires the use of a nonlinear optimisation method to search the optimum solution and its computational complexity is high. To reduce the complexity, (20) must be simplified. Here, we use the procedure outlined in [12] to do the work. To avoid the trivial all-zero solution, a constraint must be imposed. Using the constraint that

$$\sum_{k\in\Omega}\boldsymbol{w}^{\mathrm{T}}\boldsymbol{A}(k)\boldsymbol{w} = 1$$

we define the TEQ optimisation problem as

$$\text{Minimise } \boldsymbol{w}^{\mathrm{T}}\left(\sum_{k\in\Omega}\mathbf{Y}(k)\right)\boldsymbol{w},\ \text{subject to } \boldsymbol{w}^{\mathrm{T}}\left(\sum_{k\in\Omega}\mathbf{A}(k)\right)\boldsymbol{w} = 1 \tag{21}$$

From results derived previously, we have

$$\sum_{k\in\Omega}\boldsymbol{w}^{\mathrm{T}}\boldsymbol{Y}(k)\boldsymbol{w} = \boldsymbol{w}^{\mathrm{T}}\sum_{k\in\Omega}\mathrm{E}\{\lfloor\tilde{\boldsymbol{N}}_i(k)\rceil^2\}\boldsymbol{w} + \boldsymbol{w}^{\mathrm{T}}\boldsymbol{H}^{\mathrm{T}}\boldsymbol{D}_{\mathrm{I}}^{\mathrm{T}} \times \sum_{k\in\Omega}\mathrm{E}\{\lfloor\tilde{\boldsymbol{X}}_i(k)\rceil^2\}\boldsymbol{D}_{\mathrm{I}}\boldsymbol{H}\boldsymbol{w} \tag{22}$$

From the definition of $\mathrm{E}\{\lfloor\tilde{\boldsymbol{N}}_i(k)\rceil^2\}$, we can derive its closed-form expression as

$$\mathrm{E}\{\lfloor\tilde{\boldsymbol{N}}_i(k)\rceil^2\} = \sigma_\eta^2\begin{bmatrix} a_1 & b_{1,2} & \cdots & b_{1,N} \\ b_{2,1} & a_2 & \cdots & b_{2,N} \\ \vdots & \vdots & \ddots & \vdots \\ b_{N,1} & b_{N,2} & \cdots & a_N \end{bmatrix} \tag{23}$$

where

$$\begin{cases} a_i = M & \text{for all } i, \\ b_{i,j} = (M - i + j)\alpha^{(j-i)k} & \text{for } i > j \\ b_{i,j} = (M + i - j)\alpha^{(j-i)k} & \text{for } i < j \end{cases}$$

Similarly, we have $\mathrm{E}\{\lfloor\tilde{\boldsymbol{X}}_i(k)\rceil^2\}$ as

$$\sigma_{\mathrm{d}}^2\begin{bmatrix} a_1 & b_{1,2} & \cdots & b_{1,L+1} \\ b_{2,1} & a_2 & \cdots & b_{2,L+1} \\ \vdots & \vdots & \ddots & \vdots \\ b_{L+1,1} & b_{L+1,2} & \cdots & a_{L+1} \\ b_{L+2,1} + c_{L+2,1} & b_{L+2,2} & \cdots & b_{L+2,L+1} \\ b_{L+3,1} + c_{L+3,1} & b_{L+3,2} + c_{L+3,2} & \cdots & b_{L+3,L+1} \\ \vdots & \vdots & \ddots & \vdots \\ b_{M,1} + c_{M,1} & b_{M,2} + c_{M,2} & \cdots & b_{M,L+1} + c_{M,L+1} \end{bmatrix}$$
$$\begin{bmatrix} b_{1,L+2} + c_{1,L+2} & \cdots & b_{1,M} + c_{1,M} \\ b_{2,L+2} & \cdots & b_{2,M} + c_{2,M} \\ \vdots & \ddots & \vdots \\ b_{L+1,L+2} & \cdots & b_{L+1,M} + c_{L+1,M} \\ a_{L+2} & \cdots & b_{L+2,M} + c_{L+2,M} \\ b_{L+3,L+2} & \cdots & b_{L+3,M} + c_{L+3,M} \\ \vdots & \ddots & \vdots \\ b_{M,L+2} + c_{M,L+2} & \cdots & a_M \end{bmatrix} \tag{24}$$

where

$$\begin{cases} c_{i,j} = (i - j - L)\alpha^{(M+L+j-i)k} & \text{for } i > j \\ c_{i,j} = (j - i - L)\alpha^{-(M+L-j+i)k} & \text{for } i < j \end{cases}$$

The maximisation problem in (21) is known to be a Rayleigh quotient problem, and the solution can be obtained with the eigen-decomposition method. Let

$$\boldsymbol{A} = \sum_{k\in\Omega}\mathbf{A}(k),\ \boldsymbol{Y} = \sum_{k\in\Omega}\mathbf{Y}(k)$$

Using the Cholesky decomposition, we have

$$\boldsymbol{A} = \boldsymbol{A}_{\mathrm{CD}}^{\mathrm{T}}\boldsymbol{A}_{\mathrm{CD}}$$

doi: 10.1049/iet-com.2008.0133

The optimal TEQ solution to (21) is known to be

$$\boldsymbol{w}_{\text{opt}} = \boldsymbol{A}_{\text{CD}}^{-1}\boldsymbol{p}_{\min} \tag{25}$$

where $\boldsymbol{p}_{min}$ is the Eigen vector corresponding to the minimum eigenvalue of a composite matrix $\boldsymbol{A}_{\text{CD}}^{-1}\boldsymbol{Y}(\boldsymbol{A}_{\text{CD}}^{\text{T}})^{-1}$ [9]. We refer to the EMBR solved with the suboptimum method as simplified EMBR (SEMBR). The SEMBR method avoids the complicated non-linear optimisation problem. Simulations show that the TEQ designed with the SEMBR method is close to the optimum.

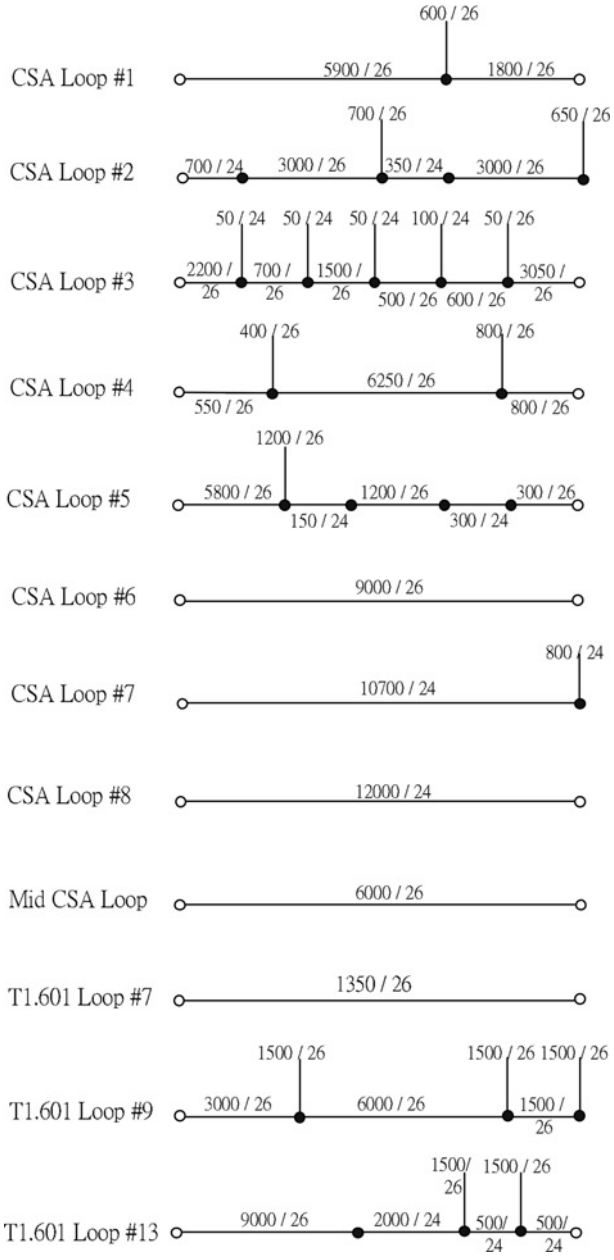

Figure 9 *Configuration of various standard test loops defined in ITU-T Recommendation G.996.1*

The numbers on a line segment represent the length (feet) and the wire gauge (American wire gauge) of the line. The left side of a loop is connected to a central office.

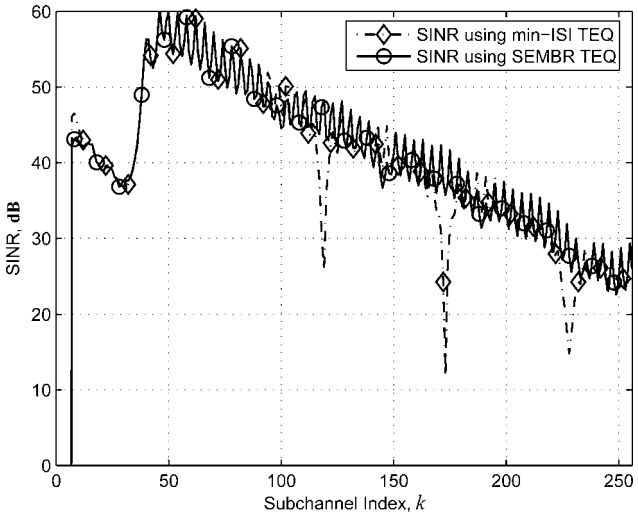

Figure 10 *SINR comparison between TEQs designed for min-ISI method and SEMBR method (N = 16, mid-CSA#6 Loop)*

5 Simulations

In this section, we report some simulation results to demonstrate the effectiveness of the proposed TEQ method. We use the 12 standard test loops defined in the ITU ADSL specification [23], including three revised resistance design (RRD) loops, eight carrier serving area (CSA) loops and one Mid-CSA loop. Fig. 9 shows the configuration of these test loops. In this figure, the numbers specified for a link represent the wire length and the wire gauge of the link. The performance of the proposed SEMBR method and that of the original min-ISI method [12] is compared. The channel noise was

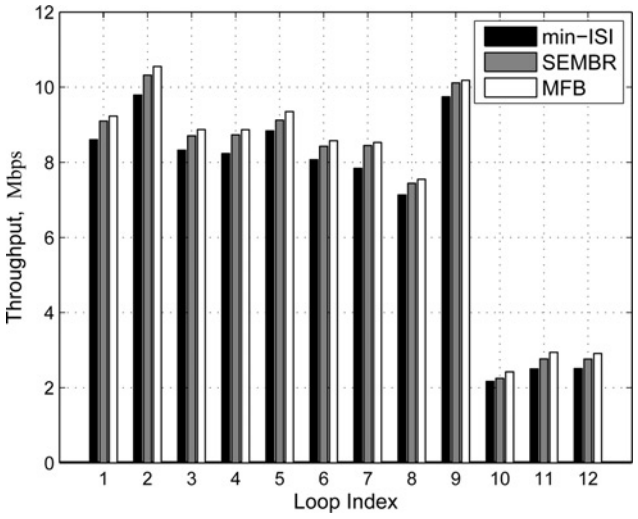

Figure 11 *Throughput comparison for TEQs designed with min-ISI and SEMBR method (N = 16)*

MFB shows upper bound with no ISI. Loop index is defined in Table 1

Table 1 Throughput for various TEQ design methods in Mbps

Loop index	Test loop	min-ISI	SEMBR	MFB
1	CSA Loop #1	8.6045	9.0972	9.2306
2	CSA Loop #2	9.7885	10.321	10.548
3	CSA Loop #3	8.3222	8.7051	8.8715
4	CSA Loop #4	8.2342	8.7314	8.8668
5	CSA Loop #5	8.8369	9.1219	9.3507
6	CSA Loop #6	8.0701	8.4261	8.5745
7	CSA Loop #7	7.8381	8.4464	8.5303
8	CSA Loop #8	7.1301	7.4443	7.5482
9	midCSA Loop	9.7429	10.114	10.182
10	T1.601 Loop #7	2.1658	2.2491	2.4220
11	T1.601 Loop #9	2.5006	2.7647	2.9412
12	T1.601 Loop #13	2.5112	2.7635	2.9090

modelled as AWGN with a flat power spectrum density of -140 dBm Hz^{-1}, and near-end-cross-talk (NEXT) noise from five integrated services digital network (ISDN) disturbers [24]. The transmit signal power was set to 23 dBm. The DFT/IDFT size, as defined in the ITU ADSL standard, is 512, and the CP size is 32 [25]. In addition, the sampling rate was set to 2.208 MHz, and the overall SNR gap Γ is 11.6 dB [26].

Fig. 10 shows the subchannel SINRs with TEQs obtained by the min-ISI and the SEMBR methods for mid-CSA loop #6. Both SINR plots are evaluated with 500 DMT symbols. As we can see, these two SINR distributions are very close. However, some nulls appear in the SINR plot associated with the min-ISI method. Bit loading in these subchannels are then seriously affected. Fig. 11 shows the throughput comparison for the DMT systems with TEQs designed by the min-ISI and SEMBR methods. All 12 test loops mentioned above were evaluated and the size of the TEQ used here was set to 16. Note that the loop index in Fig. 11 is defined in Table 1 and the table also shows the detailed throughput in Fig. 11. The matched filter bound (MFB) in Fig. 11, calculated without the ISI effect, serves as the theoretical upper bound. From the figure, we can observe that the throughput of the DMT system with the TEQ designed by the SEMBR method is consistently higher than that generated by the min-ISI method. Fig. 12 shows the frequency responses of TEQs designed with the min-ISI and SEMBR methods for CSA loop #6 and T1.601 loop #9. From the figure, we can clearly tell the difference between these two methods. The TEQ responses yielded by the proposed SEMBR method do not have the spectrum nulls as those observed from the min-ISI method. The appearance of the nulls is because of the underestimate of the noise and residual ISI powers.

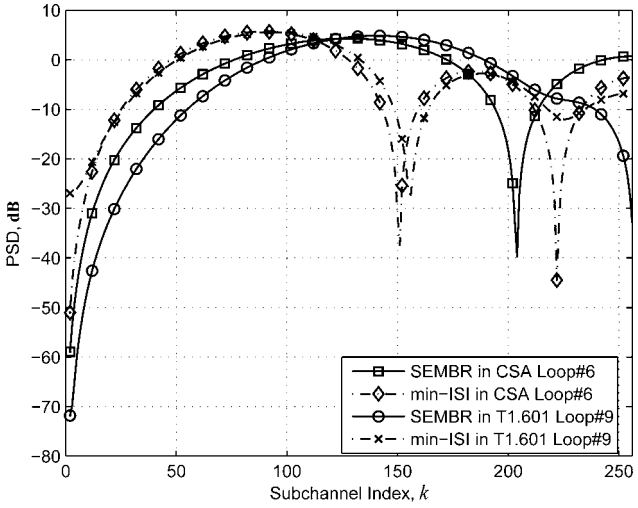

Figure 12 *TEQ frequency responses designed with min-ISI and SEMBR method (N = 16)*

6 Conclusions

The TEQ is a device used in DMT systems to combat the ISI problem. Many methods have been proposed to obtain optimum TEQs. However, we have found that these optimum TEQs are actually not optimal. This is because the noise signal, observed in a DMT symbol, does not have a CP, and the circular convolution for the noise signal and the TEQ cannot be conducted. Conventional methods ignored these phenomena, and erroneously calculate the noise and residual ISI powers of subcarriers. In this paper, we derived the correct formula for the calculation of noise and residual ISI power. It turns out that these powers are larger than those calculated by the conventional methods. Using the capacity maximisation criterion, we then propose a new

doi: 10.1049/iet-com.2008.0133

optimal TEQ design method, called the EMBR method. The EMBR method requires a constrained nonlinear optimisation solver and hence is not cost effective. To reduce the computational complexity, we then derive a simplified EMBR method, i.e. the SEMBR method. Simulations based on various ADSL standard test loops show that the proposed SEMBR method outperforms the well known min-ISI method. Furthermore, the throughput yielded by the proposed SEMBR method closely approaches the matched filter bound, which is the theoretical upper bound for the channel capacity. This clearly shows that the TEQ designed using the proposed method closely approaches the theoretical upper bound.

7 References

[1] NAKHAI M.R.: 'Multicarrier transmission', *IET Signal Process.*, 2008, **2**, (1), pp. 1–14

[2] HARA S., OKADA M., MORINAGA N.: 'Multicarrier modulation technique for wireless local area networks'. Fourth Eur. Conf. Radio Relay Syst., IEE, October 1993, pp. 33–38

[3] CHOW P.S., CIOFFI J.M., BINGHAM J.A.C.: 'DMT-based ADSL: concept, architecture, and performance'. IEE Colloquium on High speed Access Technol. Serv., October 1994, p. 3/1–3/6

[4] MOULIN F., OUZZIF M., ZEDDAM A., GAUTHIER F.: 'Discrete-multitone-based ADSL and VDSL systems performance analysis in an impulse noise environment', *IEE Proc. Sci. Meas. Technol.*, 2003, **150**, (6), pp. 273–278

[5] ITU-T Recommendation G.992.1: 'Asymmetrical Digital Subscriber Line (ADSL) Transceivers', March 1999

[6] ANSI standard T1.424: 'Very-high bit-rate Digital Subscriber Lines (VDSL) Metallic Interface, Part 3: Multicarrier Modulation (MCM) Specification', 2003

[7] CHOW J., CIOFFI J.M.: 'A cost effective maximum likelihood receiver for multicarrier systems'. Int. Conf. Commun., Chicago, June 1992, pp. 948–952

[8] FARHANG-BOROUJENY B., DING M.: 'Design methods for time-domain equalizers in DMT transceivers', *IEEE Trans. Commun.*, 2001, **49**, (3), pp. 554–562

[9] MELSA P.J., YOUNCE R.C., ROHRS C.E.: 'Impulse response shortening for discrete multitone transceiver', *IEEE Trans. Commun.*, 1996, **44**, (12), pp. 1662–1672

[10] AL-DHAHIR N., CIOFFI J.M.: 'Optimum finite-length equalization for multicarrier transceivers', *IEEE Trans. Commun.*, 1996, **44**, (1), pp. 56–64

[11] HENKEL W., TAUBOCK G., ODLING P., BORJESSON P.O., PETERSSON N.: 'The cyclic prefix of OFDM/DMT – an analysis'. Int. Zurich Seminar Broadband Commun. Access, Transm. Network, February 2002, vol. 2, pp. 1–3

[12] ARSLAN G., EVANS B.L., KIAEI S.: 'Equalization for discrete multitone transceivers to maximize bit rate', *IEEE Trans. Signal Process.*, 2001, **49**, (12), pp. 3123–3135

[13] MILOSEVIC M.: 'Maximizing data rate of discrete multitone systems using time domain equalization design'. PhD Thesis, The University of Texas at Austin, May 2003

[14] SHUR R., SPEIDEL J.: 'An efficient equalization method to minimize delay spread in OFDM/DMT systems'. Proc. IEEE Int. Conf. Commun, Helsinki, Finland, June 2001, vol. 5, pp. 1481–1485

[15] TKACENKO A., VAIDYANATHAN P.P.: 'A low-complexity eigenfilter design method for channel shortening equalizers for DMT systems', *IEEE Trans. Commun.*, 2003, **51**, (7), pp. 1069–1072

[16] L'OPEZ-VALCARCE R.: 'Minimum delay spread TEQ design in multicarrier systems', *IEEE Signal Process. Lett.*, 2004, **11**, (8), pp. 682–685

[17] MARTIN R.K., VANBLEU K., DING M. *ET AL.*: 'Unification and evaluation of equalization structures and design algorithms for discrete multitone modulation systems', *IEEE Trans. Signal Process.*, 2005, **53**, (10), pp. 3880–3894

[18] VAN ACKER K., LEUS G., MOONEN M., VAN DE WIEL O., POLLET T.: 'Per tone equalization for DMT-based systems', *IEEE Trans. Commun.*, 2001, **49**, (1), pp. 109–119

[19] VANBLEU K., YSEBAERT G., CUYPERS G., MOONEN M., VAN ACKER K.: 'Bitrate maximizing time-domain equalizer design for DMT-based systems', *IEEE Trans. Commun.*, 2004, **52**, (6), pp. 871–876

[20] KIM J., POWERS E.J.: 'Subsymbol equalization for discrete multitone systems', *IEEE Trans. Commun.*, 2005, **53**, (9), pp. 1551–1560

[21] CHEN Y.F.: 'The optimal time-domain equalization of DMT transceivers', Master thesis, Chiao Toung University, Taiwan, 2001

[22] WU W.R., LEE C.F.: 'Time domain equalization for DMT transceivers : A new result'. Proc. Intelligent Signal Process. Commun. Syst., Hong-Kong, December 2005, pp. 553–556

[23] ITU-T Recommendation G.996.1: 'Test procedures for digital subscriber line (DSL) transceivers', February 2001

[24] STARR T., CIOFFI J.M., SILVERMAN P.J.: 'Understanding digital subscriber line technology' (Prentice-Hall, Englewood Cliffs, NJ, 1999)

[25] ARSLAN G., DING M., LU B., MILOSEVIC M., SHEN Z., EVANS B.L.: 'Matlab DMTTEQ design toolbox version 3.1', The University of Texas at Austin, http:\\www.ece.utexas.edu\~bevans\projects\adsl\dmtteq\dmtteq.html

[26] CHOW P.S., CIOFFI J.M.: 'Bandwidth optimization for high speed data transmission over channels with severe intersymbol interference'. GLOBECOM'92, Orlando, December 1992, pp. 59–63

doi: 10.1049/iet-com.2008.0133